

Current Biology

Biophysical and Population Genetic Models Predict the Presence of “Phantom” Stepping Stones Connecting Mid-Atlantic Ridge Vent Ecosystems

Highlights

- Mid-Atlantic vent mussel populations are contemporarily isolated
- Population connectivity can only be maintained in a stepwise manner
- Four mussel lineages exist on the Mid-Atlantic Ridge
- Recolonization of perturbed vent localities is uncertain

Authors

Corinna Breusing, Arne Biastoch, Annika Drews, ..., Markus B. Schilhabel, Philip Rosenstiel, Thorsten B.H. Reusch

Correspondence

cbreusing@geomar.de

In Brief

Assessment of contemporary connectivity in hydrothermal vents is critical for a thorough understanding of vent biology and the mitigation of environmental impacts from deep-sea mining. In contrast to previous assumptions, Breusing et al. show that connections between mid-Atlantic vent mussel populations can only be achieved via stepping-stone habitats.

Accession Numbers

SRP076908
KU950834–KU951111
KX236334–KX236395



Biophysical and Population Genetic Models Predict the Presence of “Phantom” Stepping Stones Connecting Mid-Atlantic Ridge Vent Ecosystems

Corinna Breusing,^{1,*} Arne Biastoch,¹ Annika Drews,¹ Anna Metaxas,² Didier Jollivet,³ Robert C. Vrijenhoek,⁴ Till Bayer,¹ Frank Melzner,¹ Lizbeth Sayavedra,⁵ Jillian M. Petersen,^{5,6} Nicole Dubilier,⁵ Markus B. Schilhabel,⁷ Philip Rosenstiel,⁷ and Thorsten B.H. Reusch¹

¹GEOMAR Helmholtz Centre for Ocean Research, 24105 Kiel, Germany

²Department of Oceanography, Dalhousie University, Halifax, NS B3H 4R2, Canada

³CNRS, Sorbonne Universités, UMR 7144 CNRS-UPMC, Adaptation et Diversité en Milieu Marin, Équipe ABICE, Station Biologique de Roscoff, 29688 Roscoff Cedex, France

⁴Monterey Bay Aquarium Research Institute, Moss Landing, CA 95039, USA

⁵Symbiosis Department, Max Planck Institute for Marine Microbiology, 28359 Bremen, Germany

⁶Department of Microbiology and Ecosystem Science, University of Vienna, 1090 Vienna, Austria

⁷Institute of Clinical Molecular Biology (IKMB), Christian-Albrechts-Universität zu Kiel, 24105 Kiel, Germany

*Correspondence: cbreusing@geomar.de

<http://dx.doi.org/10.1016/j.cub.2016.06.062>

SUMMARY

Deep-sea hydrothermal vents are patchily distributed ecosystems inhabited by specialized animal populations that are textbook meta-populations. Many vent-associated species have free-swimming, dispersive larvae that can establish connections between remote populations. However, connectivity patterns among hydrothermal vents are still poorly understood because the deep sea is undersampled, the molecular tools used to date are of limited resolution, and larval dispersal is difficult to measure directly. A better knowledge of connectivity is urgently needed to develop sound environmental management plans for deep-sea mining. Here, we investigated larval dispersal and contemporary connectivity of ecologically important vent mussels (*Bathymodiolus* spp.) from the Mid-Atlantic Ridge by using high-resolution ocean modeling and population genetic methods. Even when assuming a long pelagic larval duration, our physical model of larval drift suggested that arrival at localities more than 150 km from the source site is unlikely and that dispersal between populations requires intermediate habitats (“phantom” stepping stones). Dispersal patterns showed strong spatiotemporal variability, making predictions of population connectivity challenging. The assumption that mussel populations are only connected via additional stepping stones was supported by contemporary migration rates based on neutral genetic markers. Analyses of population structure confirmed the presence of two southern and two hybridizing northern mussel lineages that exhibited a substantial, though incomplete, genetic differentiation. Our study provides insights

into how vent animals can disperse between widely separated vent habitats and shows that recolonization of perturbed vent sites will be subject to chance events, unless connectivity is explicitly considered in the selection of conservation areas.

INTRODUCTION

The deep ocean hosts one of the most intriguing environments on our planet—hydrothermal vents [1]. These systems result from the penetration of oxygenated seawater into the oceanic crust, where water-rock interactions produce chemically altered fluids that reemerge from the seabed and lead to the precipitation of polymetallic sulfide deposits [2]. In the absence of sunlight, specialized microorganisms oxidize reduced compounds from the hydrothermal fluids to generate energy for carbon fixation [3]. These chemosynthetic microbes often live in symbioses with vent-dwelling invertebrate animals, creating oases of life in the otherwise sparsely populated deep-sea environment [1]. Similar to other marine invertebrates, many vent species pass through a free-swimming larval phase that can establish and maintain connections among geographically separated vent populations. Several physical and biological factors influence patterns of larval dispersal [4] and the degree of effective population connectivity. Effective population connectivity is defined as the successful recruitment of settlers, which includes dispersal. The processes controlling larval exchange among vent populations separated by hundreds to thousands of kilometers are poorly understood. Dispersal and connectivity are critical for maintaining the stability of ecosystems and their recovery potential from environmental disturbance. Increasing interests in commercial mining of precious metals from vent-associated seafloor massive sulfides (SMSs) are currently posing the largest immediate threat to hydrothermal ecosystems in the deep sea [5].

Vent populations are prime examples for meta-populations that come and go depending on the transient nature of the

hydrothermal fluids [6]. Vent organisms have evolved characteristic life-history adaptations such as fast growth, early sexual maturity, and opportunistic adjustments of the pelagic larval duration (PLD) [7], making them more resilient to anthropogenic perturbations. Nevertheless, a rigorous quantification of effective connectivity and genetic population structure of vent species is still lacking, hampering the development of efficient management plans for conservation [8].

Since direct measurements of larval dispersal are logistically challenging [9], two major techniques are used to quantify migration between populations indirectly: molecular characterization of gene flow and biophysical models based on Lagrangian analyses, i.e., individual particle tracking in space and time [10]. The term “biophysical” refers to the combination of ocean current models with the incorporation of biological parameters (e.g., timing of larval release and duration of larval life) to obtain large ensembles of passive drift trajectories that are representative of pelagic larval dispersal. Both methods have their limitations [10]. The chosen molecular markers may not sufficiently resolve contemporary population structure. In addition, they might fail to detect direct connectivity and lead to wrong assignments of source populations, if intermediate habitats have not been sampled. By being able to simulate multiple larval releases on ecological timescales, biophysical modeling analyses can avoid issues with sampling gaps. However, such simulations will be problematic if the numerical ocean and particle-tracking models have limited spatiotemporal resolution or lead to inaccurate assumptions due to under-parameterization [10, 11]. A combination of approaches is therefore warranted, yet few studies have used both methods to cross-validate results [12–14].

Mussels of the genus *Bathymodiolus* (Bivalvia: Mytilidae) are key members of animal communities at chemosynthetic ecosystems worldwide. In many vent environments, they represent foundation species that form dense mussel beds that serve as habitats and settlement substrates for other vent-associated organisms [15]. Like their shallow-water relatives, bathymodiolin mussels are sessile as adults and have a planktonic larval stage that enables exchange among populations. Arellano and Young [16] concluded that larvae of the cold-seep mussel *B. childressi* are able to delay the timing of metamorphosis and extend their PLD to a maximum length of 13 months. Because *Bathymodiolus* veligers can be transported away from the seafloor by passive entrainment in hydrothermal plumes [17] and migrate vertically during their ontogenetic development [18], larvae may be dispersed over large distances in upper ocean currents. How the potential for long-distance dispersal actually shapes population structure and connectivity in these deep-sea organisms is not understood.

On the Mid-Atlantic Ridge (MAR), four (sub-)species of *Bathymodiolus* dominate the vent fauna [19, 20]: in the north, *B. azoricus* occurs at vents on the Azorean Triple Junction (NMAR), and *B. puteoserpentis* occurs along the central MAR (MMAR) [19]. These species hybridize locally at the intermediate Broken Spur vent field [21]. In the south, two unnamed closely related *Bathymodiolus* species were recently described from hydrothermal vents at 5°S and 9°S [20]. Evidence from phylogeographic analyses of the *COI* mitochondrial gene suggested that all four MAR *Bathymodiolus* (sub-)species form a monophyletic group that split after separation from their western Atlantic

cold-seep ancestors, the *B. boomerang* complex [20]. Colonization of the MAR by *Bathymodiolus* most likely happened at the northern ridge segments, with subsequent expansions into the southern Atlantic [20].

In this study, we applied 100 high-resolution genetic markers and Lagrangian analyses of larval dispersal based on a realistic North Atlantic Ocean general circulation model (OGCM) to assess patterns of effective connectivity and genetic subdivision in these mussels (see Table S1 and Figure 1 for sampling sites and abbreviations). In contrast to expectations from long PLDs, our data suggest that migration between *Bathymodiolus* populations from currently known vent sites can only be achieved via so far undiscovered chemosynthetic habitats (“phantom” stepping stones).

RESULTS

Genetic Structure and Divergence of MAR Mussels

To evaluate gene flow among populations, we applied Bayesian inference analyses in the program STRUCTURE [22], using all available molecular markers (90 SNPs, nine microsatellites [MSATs], and mitochondrial *ND4*). Following the conservative ΔK correction by Evanno et al. [23], we found evidence for one southern and two northern genetic clusters (K) on the MAR ($K = 3$; Figure 2A). However, this approach might only reveal the most parsimonious partitioning [24] provided that all individuals can be specifically assigned to the defined groups under the assumption of Hardy-Weinberg equilibrium. As we expected further genetic structuring, we inspected non-significant STRUCTURE results based on higher K values. These investigations revealed an additional subcluster in the southern Atlantic ($K = 4$; Figure 2B)—in concordance with pairwise F_{ST} index calculations (Table 1) and previous species delineations [19, 20]. Among STRUCTURE clusters, all pairwise F_{ST} values were significant and indicated a substantial genetic differentiation (Table 1: $F_{ST} = 0.3212$ – 0.8388). By contrast, populations within clusters were genetically undifferentiated (i.e., populations of *B. azoricus* comprising MG, LS, and RB; and populations of *B. puteoserpentis* comprising SP, IR, QS, and SM). In agreement with previous findings [21], the BS vent field hosted a mixed mussel population, resulting from hybridization between the two northern clusters of *B. azoricus* and *B. puteoserpentis* (Figure 2). Consequently, the genetic differentiation of BS to *B. azoricus* and *B. puteoserpentis* was lower than that of other sites, while divergence from the southern clusters was in the range of the *B. puteoserpentis*-*B. sp.* 5°S and *B. puteoserpentis*-*B. sp.* 9°S pairs (Table 1).

Overall, the absence of genetic structure within clusters, the occurrence of hybridization, and the incomplete differentiation among clusters demonstrate that gene flow occurs, particularly in the northern part of the MAR.

Contemporary Gene Flow

To assess present gene flow between the sampled vent localities, we calculated contemporary migration rates in the program BayesAss [25]. Since loci under natural selection would most likely bias these estimates, we used 44 polymorphic molecular markers (36 SNPs and eight MSATs) that were evidently neutral based on F_{ST} outlier tests (Tables S2, S3, and S4). Our results

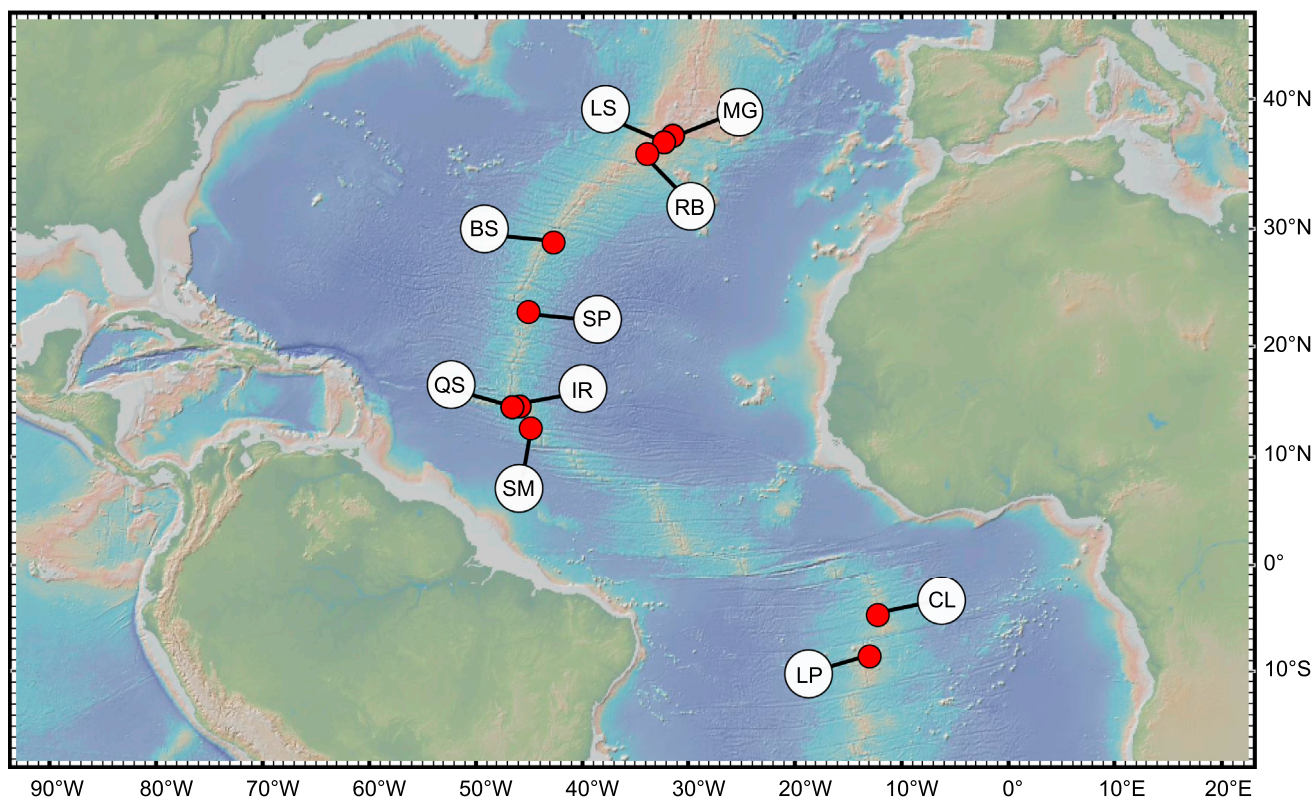


Figure 1. Geographic Map of the Sampled *Bathymodiolus* Locations along the MAR

MG, Menez Gwen; LS, Lucky Strike; RB, Rainbow; BS, Broken Spur; SP, Snake Pit; IR, Irina; QS, Quest; SM, Semenov; CL, Clueless; LP, Lilliput. The image was produced with GEOMAPAPP v3.6.0 (<http://www.geomapapp.org>) and INKSCAPE v0.48 (<https://inkscape.org>). See also Table S1.

implied a high amount of local retention for each region (fraction of individuals derived from source vent ≥ 0.7084 ; Figure 3; Table S5). No direct connection between sites was observed within one generation. The only exception was the BS locality, where our analyses indicated immigration of *B. puteoserpentis* from the MMAR region (0.2488; Figure 3; Table S5). This pattern was generally consistent, regardless of whether the pooled NMAR *B. azoricus* hosted vents (MG, LS, and RB) and MMAR *B. puteoserpentis* hosted vents (SP, IR, QS, and SM) were used or whether only one vent from each of the two pools was included in the runs (exception: some migration rates became marginally significant when only SM was included in the analyses). This result indicates that the model simulations with pooled datasets were free of bias and can be used as basis for data interpretation.

Larval Dispersal via Biophysical Modeling

In addition to our molecular approaches, we performed particle-tracking analyses to assess the potential contemporary connectivity among the MAR localities. Unconstrained estimates of dispersal suggested that passive larval drift is potentially widespread, although transport to distant points from the release position appeared to be extremely unlikely (Figure 4; $\leq 0.2\%$). Generally, larval dispersal depends on the depth and bathymetric setting of each vent. At LS, larval drift had a southwest-northeast orientation, consistent with the bi-directionality of currents simulated at the LS vent field (Figure S1). However,

based on our estimated dispersal kernels (i.e., the probability distribution as a function of geographic distance), there was no significant spatial overlap of kernels between the known vent sites MG, LS, and RB, even with a PLD of 1 year (Figure 5). For releases from these sites and assuming no mortality, median probabilities were less than 6% that passively drifting larvae could be within reach of a hydrothermal plume (≤ 400 meters above bottom [mab]) and would thus be able to sense a potential vent locality for settlement. Very rarely, likelihoods increased to $\sim 17\%$ (Figure 5; median and maximum values for releases from RB), but only at or close to the source vent. Probabilities of arrival at more distant sites were reduced to zero before another known vent field was reached. These results indicated that intermediate, presently unknown chemosynthetic habitats must exist to enable connectivity between known vents. To assess the required spacing of these localities and to evaluate whether the observed lack of direct connectivity was a consistent pattern along the MAR, we performed additional model runs for hypothetical vent fields placed at 100-km intervals along the ridge axis. In these simulations, dispersal directions and distances varied greatly among release sites and years, without a predictable pattern in the underlying oceanographic structures for the known vent sites MG, LS, and RB. This indicates that dispersal events were largely stochastic. Despite temporal variability in larval transport, median effective dispersal distances never exceeded 150 km during a PLD of 1 year (Figure 5A; Table 2). These estimates were further reduced (< 110 km)

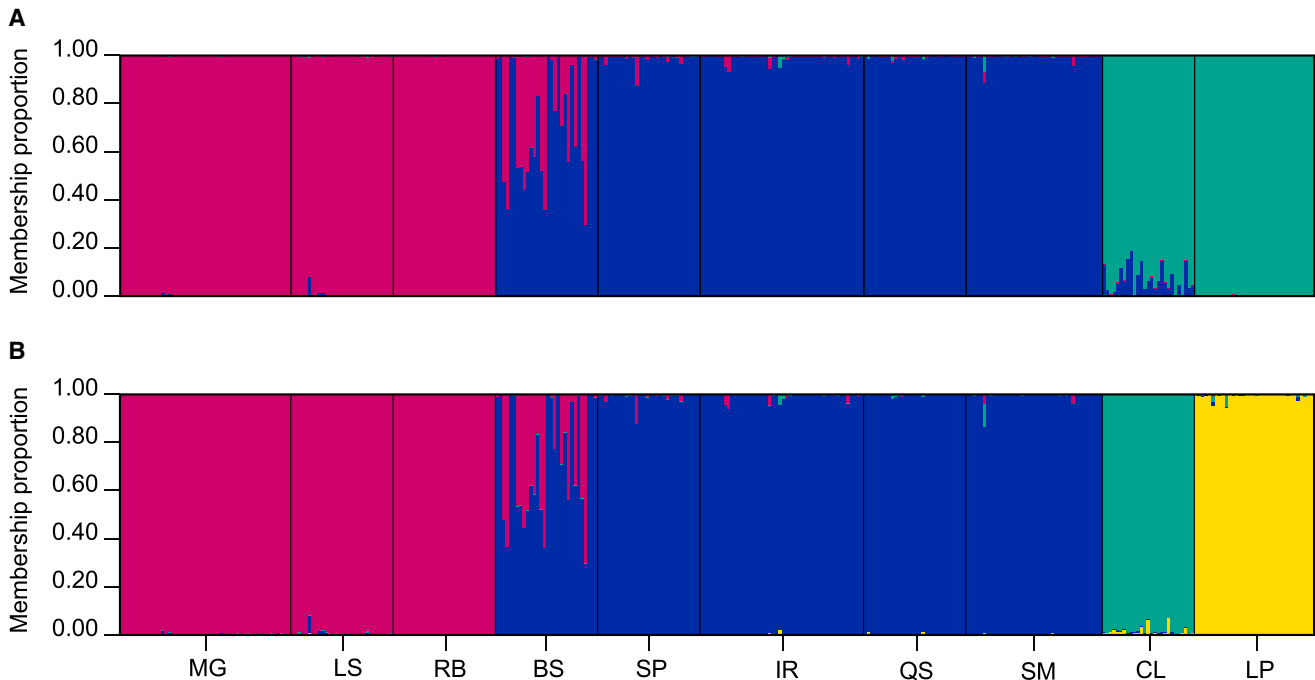


Figure 2. Structure of *Bathymodiolus* Populations along the MAR

$K = 3$ genetic groups (A) and $K = 4$ genetic groups (B). Different groups are indicated by different colors. Each vertical line represents one individual, and color ratios show the inferred proportional membership to one or more clusters.

when larvae dispersed for only 6 months (Figure 5B; Table 2). Median travel distances across all vents were 51–86 km and 21–26 km for 1-year and 6-month dispersal, respectively (Table 2). Depending on the starting position, a few larvae sometimes reached remote vent fields at distances of up to 200 km (6 months) or 400 km (1 year), but such events seemed to follow no clear pattern (Table 2).

DISCUSSION

Hydrothermal vents host specialized biological communities that are solely based on chemosynthesis. At the same time, they are textbook examples of isolated meta-populations that depend critically on the processes assuring both connectivity and re-colonization upon natural or upcoming anthropogenic disturbances. Because *Bathymodiolus* mussels are foundation species and ecosystem engineers at hydrothermal vents [15], their repopulation potential is critical to ecosystem recovery, as disturbance through deep-sea mining is imminent [5, 8].

Here we used high-resolution particle-tracking analyses and estimates of recent genetic migration rates to infer the degree of contemporary connectivity between vent mussel populations along the MAR. Although differences in the applied algorithms and the underlying assumptions prevent quantitative comparisons, both methods suggested that migration among presently known vent fields is unlikely to happen within a single generation. Despite spatiotemporal variation in dispersal patterns, our biophysical model suggested that recipient localities typically do not lie more than 21–26 km or 51–86 km away from natal local-

ities, depending on the duration of larval drift. For each vent site, median dispersal distances never exceeded 110–150 km. This is a surprising result given that the long PLD of *Bathymodiolus* [16] should enable transport to much more distant sites and keeping in mind that passive transport models often overestimate dispersal distances for species with long PLDs [26]. Moreover, our simulations did not include any sources of mortality during dispersal or other biotic or abiotic processes that can negatively affect larval transport and recruitment [4]. Larval survival in the plankton has not been measured for most benthic invertebrates, but it is expected to be low (<10%) [27]. Lenihan et al. [28] showed that dense patches of the mussel *B. thermophilus* significantly reduced the number of settlers or surviving recruits through inter- or intra-specific competition and predation. Larval behavior, such as vertical migration and active swimming, can affect local retention and long-distance dispersal in a number of species, including cold-seep *Bathymodiolus* [11, 18]. Although vertical current velocities are similar to larval swimming speeds (a few 10^{-1} to 10^{-2} mm/s) [29] and could enable mussel larvae to move toward the surface, it is so far unknown whether veligers of MAR *Bathymodiolus* perform these migrations and whether they could survive depressurization during ascent. Given these uncertainties and the fact that the OGCM is limited in representing turbulence within the horizontal and vertical grid resolution, we did not attempt to integrate larval behavior into our simulations.

Our findings indicate that additional vent fields or other chemosynthetic habitats must be present along the ridge axis to allow connectivity among known MAR vent localities. These results agree with current predictions on the abundance of

Table 1. Pairwise Genetic and Geographic Distances between Sampled Localities

	<i>B. azoricus</i> (NMAR)			Hybrid	<i>B. puteoserpentis</i> (MMAR)				<i>B. sp. 5°S</i>	<i>B. sp. 9°S</i>
	MG	LS	RB	BS	SP	IR	QS	SM	CL	LP
MG	*	89.73	277.19	1,446.12	2,052.06	2,882.49	2,882.55	3,006.67	5,120.23	5,581.76
LS	-0.0002	*	187.84	1,356.83	1,962.55	2,796.01	2,796.07	2,920.70	5,095.01	5,551.66
RB	0.0032	0.0005	*	1,169.00	1,778.12	2,622.75	2,622.81	2,748.98	5,066.30	5,511.82
BS	<i>0.4743</i>	<i>0.4362</i>	<i>0.4456</i>	*	666.35	1,606.94	1,606.96	1,743.12	4,996.86	5,356.16
SP	<i>0.6575</i>	<i>0.6325</i>	<i>0.6421</i>	<i>0.0714</i>	*	953.50	953.50	1,090.63	4,713.82	5,018.75
IR	<i>0.6719</i>	<i>0.6519</i>	<i>0.6595</i>	<i>0.1054</i>	-0.0002	*	0.14	137.15	4,197.82	4,417.46
QS	<i>0.6822</i>	<i>0.6609</i>	<i>0.6703</i>	<i>0.0967</i>	-0.0005	-0.0019	*	137.15	4,197.94	4,417.58
SM	<i>0.6890</i>	<i>0.6705</i>	<i>0.6791</i>	<i>0.1083</i>	0.0032	-0.0003	0.0048	*	4,132.14	4,337.44
CL	<i>0.7728</i>	<i>0.7553</i>	<i>0.7631</i>	<i>0.5094</i>	<i>0.5433</i>	<i>0.5539</i>	<i>0.5570</i>	<i>0.5606</i>	*	532.97
LP	<i>0.8362</i>	<i>0.8323</i>	<i>0.8388</i>	<i>0.6455</i>	<i>0.6806</i>	<i>0.6788</i>	<i>0.6935</i>	<i>0.6940</i>	<i>0.3212</i>	*

Genetic distances are measured as F_{ST} and are given below the diagonal, and geographic distances are measured in kilometers and are given above the diagonal. F_{ST} calculations are based on the combined dataset of 90 SNPs and nine MSATs. Significant F_{ST} values after p value correction are shown in italics ($\alpha = 0.014$). MG, Menez Gwen; LS, Lucky Strike; RB, Rainbow; BS, Broken Spur; SP, Snake Pit; IR, Irina; QS, Quest; SM, Semenov; CL, Clueless; LP, Lilliput.

SMS deposits and hydrothermal systems on the MAR, which are thought to occur at least every 30–125 km on the northern MAR and every 112–230 km on the southern MAR [30]. Recent evidence from nephelometric and oxidation-reduction potential sensing techniques suggests an even closer spacing for ridge systems worldwide, indicating that vent abundances are much higher than previously assumed [31]. Although the MAR has been intensively searched for thermal anomalies and mapped with video surveys, small, diffusive vents are difficult to detect and might have been overlooked. For example, mussels described as *B. aff. azoricus* were sampled from Lost City, an off-axis peridotite-hosted vent located at 30°N latitude [32], and a diffusive vent site hosting mussels was recently discovered 5 km from MG using multibeam echosound mapping (<http://irvents-new3.who.edu/ventfield/bubblon>). Alternatively, gene flow among *Bathymodiolus* populations could have been enabled via hydrothermal systems that are now extinct.

The plausible existence of such “phantom” stepping stones could explain the lack of genetic structure between the relatively close populations within *Bathymodiolus* species and for the occurrence of a hybrid zone. Greater spatial and temporal gaps in the frequency of such stepping stones might then account for the substantial genetic differentiation of mussel localities between geographic regions. Likewise, “phantom” stepping stones could explain an observed discrepancy between expectations from the biophysical model and estimates from the BayesAss analyses that showed direct migration from the *B. puteoserpentis* hosted vents to BS. The BayesAss algorithm assumes that all source localities have been sampled [25], which would not be the case if additional vent populations exist between the known MAR sites. Such a situation would lead to an adjustment of population allele frequencies between the reported *B. puteoserpentis* locations and BS and therefore cause false signals of direct connectivity. The “phantom” stepping stone hypothesis assumes that the model predictions of median dispersal distances are generally correct and applicable to the rest of the MAR, which awaits further testing and spatial

extensions of the OGCM high-resolution grid. In particular, the fact that the *B. azoricus* hosted localities MG, LS, and RB were genetically undifferentiated could indicate that the present model results are inaccurate. Alternatively, the present genetic markers might have been inappropriate to detect population structure within taxa because they were designed to work across species, which required tradeoffs to detect significant intra-specific variation. Resolving these issues requires future development of genome-wide markers and ground truthing of the OGCM at abyssal depths, for example via drifter releases in the field [33].

Our work adds to the growing body of literature that uses both biophysical modeling and population genetic methods to assess connectivity of marine species [12–14]. This combined approach is of particular value as it can compensate individual limitations of the two techniques, thereby leading to better estimates of connectivity—a benefit that is becoming increasingly relevant for environmental management purposes [14]. Despite present uncertainties, our results have important ramifications for conservation strategies in the Atlantic Ocean. They suggest that recovery of hydrothermal ecosystems after impacts by SMS mining will not be achieved if contemporary connectivity and recolonization potential are neglected in the design of marine protected areas (MPAs). Although the development of effective measures for biodiversity conservation at mid-Atlantic vents is in its infancy, the International Seabed Authority has already provided licenses for exploration to France and Russia, and interest in exploitation of abundant SMS deposits along the MAR is increasing [34]. Despite the potential resilience of vent communities to single mining events, it is unlikely that hydrothermal ecosystems will easily recover from large-scale commercial exploitation activities, as several environmental impacts are unpredictable [8]. Anthropogenic disturbances might be particularly damaging for vent communities on slow-spreading ridges such as the MAR, where natural destructive events are comparatively rare and species might not be adapted to frequent perturbations [8]. With a conservative PLD estimate of 6 months, a MPA network consisting of individual conservation areas with

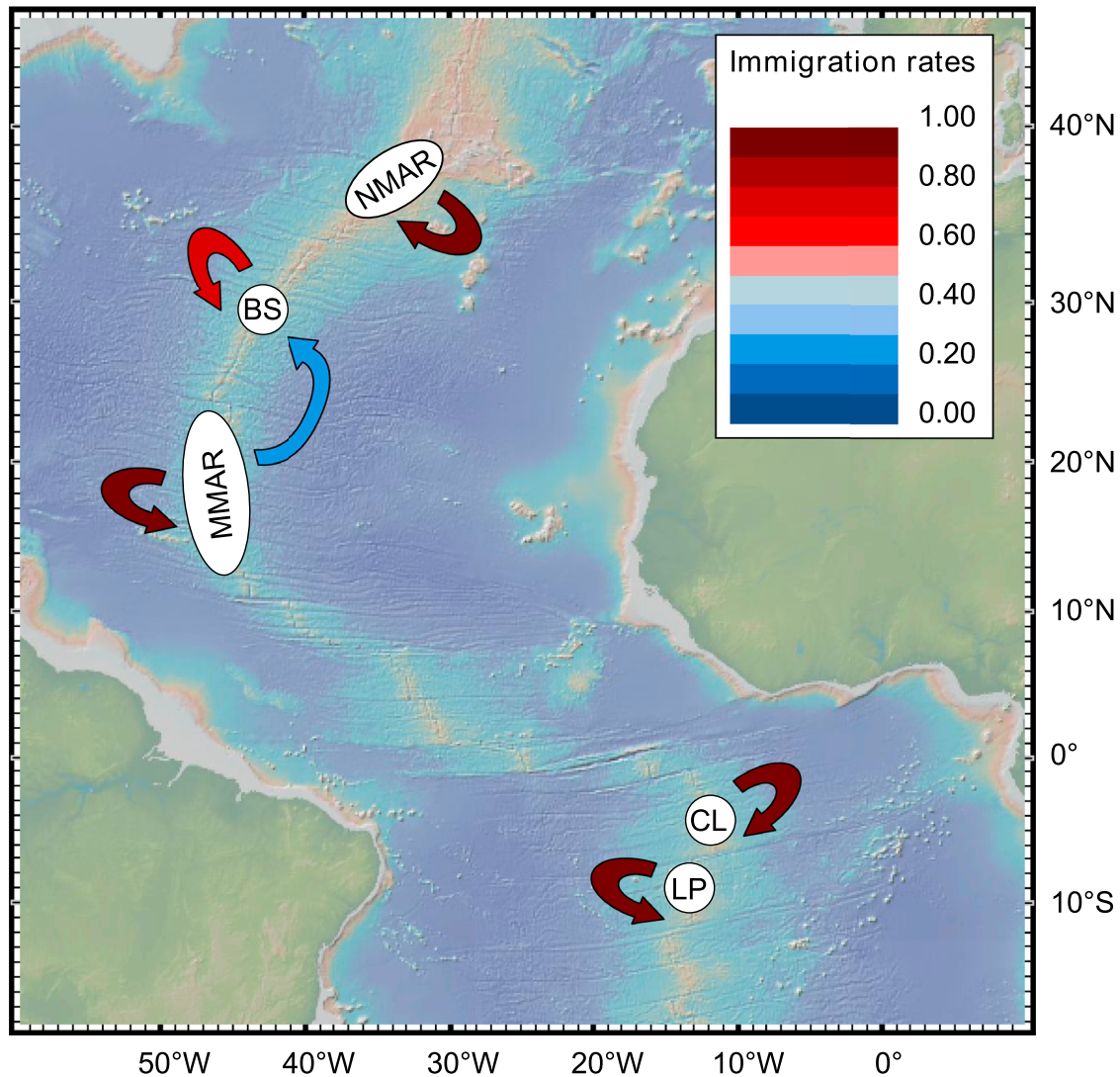


Figure 3. Contemporary Connectivity between *Bathymodiolus* Localities Based on 44 Neutral Molecular Markers

Migration rates are shown as the fraction of self-recruits within regions or immigrants per generation from another locality. NMAR, MG, LS, and RB; BS, Broken Spur; MMAR, SP, IR, QS, and SM; CL, Clueless; LP, Lilliput. See also Table S5.

region-dependent sizes and a spacing of less than 21–26 km would seem advisable to ensure repopulation of perturbed sites, at least for *Bathymodiolus* mussels. Our model data suggested that larvae can episodically reach vent fields at distances of 200–400 km, which might be sufficient to sustain long-lived, temporarily stable vent communities of the MAR. However, as these long-range dispersal patterns were unpredictable and vent dynamics are still poorly understood, these estimates are an inappropriate basis for MPA design. In general, the dispersal distances observed in our study would most likely allow population connectivity within a few decades. Interestingly, these time-scales seem to be very different from those suggested for vent systems in western Pacific back-arc basins, where connectivity is expected within hundreds to thousands of years [33]. This discrepancy is most likely explained by the linear topography and advective system of mid-ocean ridges compared to the

discontinuous nature of back-arc basins, where flow is largely constrained.

For environmental management plans for the MAR to be refined, further studies including taxa with different life-history strategies than bathymodiolin mussels are necessary. For example, vent species with shorter PLDs than *Bathymodiolus*, such as several polychaetes and gastropods [35], may disperse over much smaller distances and may require more closely spaced and/or larger MPAs for effective conservation. Closer spacing of MPAs would allow species to disperse across areas devastated by mining and reach a new protected zone, and larger MPAs would promote sustainability of populations within the conservation area. Recent biophysical models for deep-sea larvae in the Gulf of Mexico and western Pacific showed that dispersal distance is significantly correlated to PLD, which would make species with short larval periods particularly

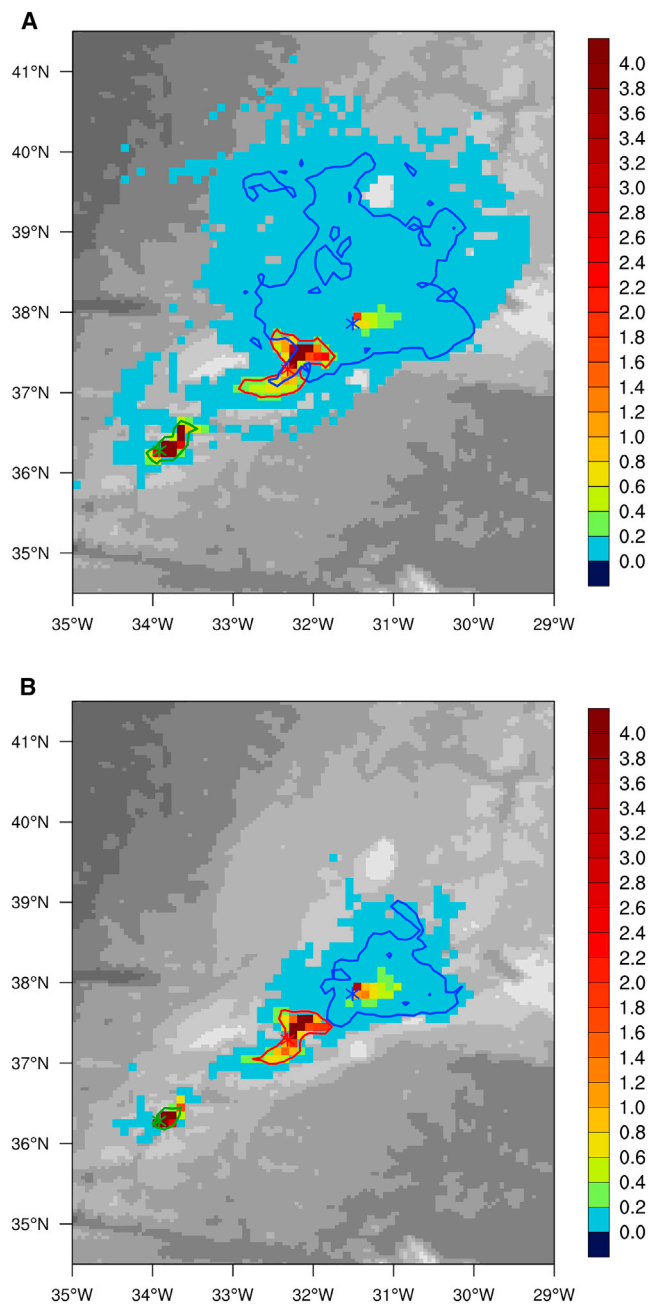


Figure 4. Simulated 10-Year-Median Dispersal Probabilities for the Respective Dispersal Periods

Probabilities are shown as percent per grid point (sum over whole water column) for annual releases from MG (blue star), LS (red star), and RB (green star) between 1998 and 2007, overlaid on VIKING20 model bathymetry. Contour lines denote areas that contain 95% of released larvae with respect to median probabilities. 1-year dispersal and (A) 6-month dispersal (B) are shown.

vulnerable to human impact [36], unless sufficiently large MPAs are in place. In contrast to the MAR, at the East Pacific Rise, propagule flux models showed that the number of exchanged migrants decreased logarithmically with increasing traveling time due to periodic current reversals along the ridge axis [37]. Independent of the marine region under study, the identification

of species with the shortest dispersal distances and accurate mapping of intermediate vent sites will be critical for the development of successful management plans to mitigate anthropogenic influences on hydrothermal ecosystems. Furthermore, accurate assessment of species composition, richness, and endemism at target mining sites will be necessary to assign appropriate source localities for repopulation and define areas where conservation will be of utmost priority [38].

EXPERIMENTAL PROCEDURES

Samples

Mussel specimens were obtained using remotely operated vehicles from ten vent localities on the MAR between 1997 and 2013 (Table S1; Figure 1). Depths of the sampling sites ranged between 813 m and 3,480 m. Most specimens were dissected upon arrival at the surface and immediately stored at -20°C to -80°C , preserved in RNAlater (-80°C), or frozen whole (-20°C to -80°C). Individuals from the BIOBAZ 2013 cruise were kept alive at GEOMAR Helmholtz Centre for Ocean Research Kiel before being dissected and frozen at -80°C . Mussels from LP (M78/2 319/8) were preserved in situ with RNAlater, using the DIE FAST fixation chambers of MPI Bremen. Sampling permissions were obtained, where relevant, for the cruises in which the samples were collected. Cruises and ROV dives for all samples are given in Table S1.

RNA Extraction and High-Throughput Transcriptome Sequencing

To develop SNP and MSAT markers for population genetic analyses, we sequenced and assembled reference transcriptomes of five to six individuals of each *Bathymodiolus* (sub-)species (MG, *B. azoricus*; IR, *B. puteoserpentis*; CL, *B. sp. 5°S*; LP, *B. sp. 9°S*; Table S1; Figure 1) that have been described from the MAR [19, 20]. We used tissue pieces from the gill and the inner and the outer mantle of each individual, except for the samples from LP, where only gill tissues were available. RNA was extracted and purified using the RNeasy Mini Kit (QIAGEN) according to manufacturer's instructions for spin technology with slight modifications (Supplemental Experimental Procedures). Purified, high-quality RNA was poly(A)-enriched (exception: LP samples) to construct barcoded libraries that were sequenced on an Illumina HiSeq 2000 platform at the Institute of Clinical Molecular Biology using a 2×101 -bp paired-end protocol (Supplemental Experimental Procedures).

De Novo Transcriptome Assembly

Paired-end sequencing resulted in an average of about 75 million paired-end reads per library. Raw reads were pre-processed using a combination of quality checking (FASTQC v0.10.1; <http://www.bioinformatics.babraham.ac.uk/projects/fastqc/>), read filtering (FASTQ_ILLU-MINA_FILTER v0.1; http://cancan.cshl.edu/labmembers/gordon/fastq_illumina_filter/), and trimming (Flexbar v2.4 [39]). De novo assemblies of digitally normalized reads (30–50 \times coverage) were constructed for each species with Trinity r20140413 [40]. Putative assembly artifacts were excluded by filtering out lowly expressed contigs (FPKM < 1) that did not have an open reading frame or a BLAST hit in public sequence databases. Redundant contigs ($\geq 99\%$ identity) were clustered with CD-HIT-EST v4.6.1 [41] (Supplemental Experimental Procedures; Table S6).

SNP Marker Design

Reads from all individuals were mapped against the *B. azoricus* transcriptome, which we chose as reference for inter-specific marker design. SNP calling and filtering was done using VarScan v2.3.7 [42] and Reads2SNP v2.0 [43]. Paralogous SNPs were excluded by blasting the SNP positions against an unpublished *B. azoricus* genome (D.J., T. Takeshi, N. Satoh, and A. Tanguy, *Bathymodiolus* genome JST project, unpublished data; Supplemental Experimental Procedures). Although the genome has not been completely assembled yet, our preliminary investigations showed that the SNP markers were widely distributed across different scaffolds. This indicates that our analyses should not be influenced by physical linkage. After successful in silico primer tests with the Fluidigm D3 system, 94 SNP Type Assays were ordered for

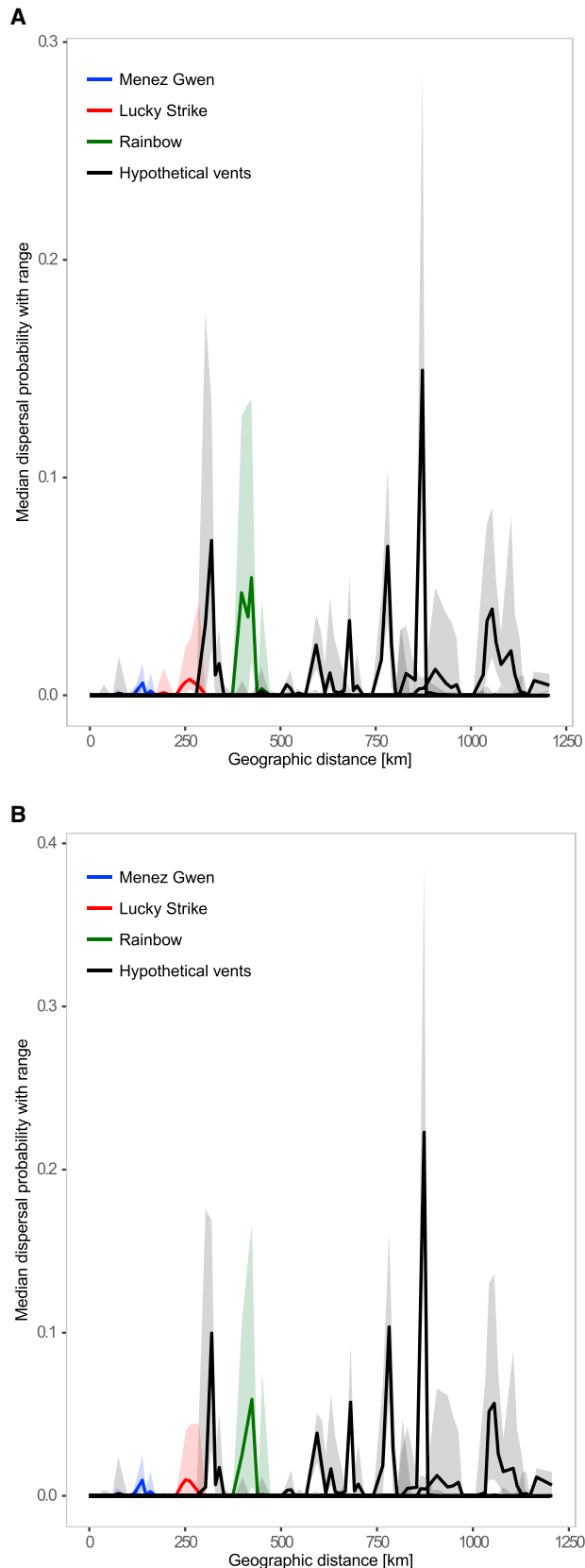


Figure 5. Median Dispersal Kernels with Maximum and Minimum Values for the Known Vents MG, LS, and RB and for Ten Hypothetical Vent Sites along the MAR

Geographic distance was measured from a reference point at 38.70°N. For the calculation of probability densities, only larvae that were within 400 meters above bottom (mab) during their planktonic period of (A) 1 year and (B) 6 months were included. Connectivity between populations is achieved if the dispersal kernel from one vent reaches over the location of another vent with probabilities >0.

genotyping. Of these, four SNPs had to be discarded due to ambiguous scoring or poor amplification (Table S2).

MSAT Marker Design

MSATs were called from the *B. azoricus* de novo transcriptome using TRF v4.07b [44]. Transcriptomes or EST libraries are commonly used as sources for MSAT development, especially when transferability to other taxa is necessary [45]. To enable cross-species marker design, we compared the MSAT contigs to all other *Bathymodiolus* transcriptomes using NCBI BLAST v2.2.29+ [46]. Candidate contigs were multiple aligned in Geneious v8.1.3 (<http://www.geneious.com>) with the Geneious alignment pairwise algorithm and inspected for conserved regions within 150 bp upstream and downstream of the repeat motif. Primers were designed in Primer3Web v4.0.0 [47] and were ordered from Metabion and Applied Biosystems. After wet testing, we selected three primer triplexes for genotyping (Table S3; Supplemental Experimental Procedures).

DNA Extraction and Genotyping

Protocols for DNA extraction, PCR procedures, and genotyping analyses are described in the Supplemental Experimental Procedures and Tables S2 and S3. For all genotyping and statistical analyses, we used at least 30 individuals per vent location.

Genetic Structure and Differentiation

We used STRUCTURE v2.3.4 [22] to infer the number of genetic groups K in our sample set. To obtain accurate insights into population structure, we incorporated information from all available markers and used a combination of different marker types (90 SNPs, nine MSATs, and *ND4*). The admixture model with correlated allele frequencies was run for $K \leq 12$, with ten replications performed for each value. In addition, we quantified the genetic differentiation between the ten sampled localities by calculating pairwise F_{ST} (SNPs and MSATs) values in Arlequin v3.5.1.2 [48] (Supplemental Experimental Procedures).

F_{ST} -Outlier Test

To assess the selective neutrality of the SNP markers for immigration rate estimation, we determined F_{ST} -outlier loci by running BayeScan v2.1 [49] on different data subsets (Supplemental Experimental Procedures) with recommended parameter settings and a q value threshold of 0.1. Note that in hybridizing species, gene introgression can produce the same pattern as divergent selection. Therefore, some outliers might be misidentified as adaptive. 75 SNPs were found to be neutrally evolving (Table S4), 39 of which were discarded due to near fixation ($\geq 95\%$) of the same allele in more than half of the populations (Table S2). The remaining 36 SNPs were combined with the eight most polymorphic MSATs (i.e., excluding c64270_g3_i1) for contemporary gene flow analyses. We used this conservative approach as loci under natural selection or with a high degree of fixation will largely underestimate migration rates.

Contemporary Gene Flow

To determine the occurrence and direction of migration between vent sites over the last two generations, we implemented Bayesian assignment methods in BayesAss v3.0 [25]. Our approach mirrored the one described in Breusing et al. [50], except that we used the following parameters to achieve the recommended acceptance rates (20%–60%) for changes in migration rate, inbreeding coefficient, and allele frequencies: $-m$, 0.10–0.15; $-f$, 0.50–0.60; and $-a$, 0.30–0.40. To ensure reliability of the estimates, we had to pool

Table 2. Dispersal Distances in Kilometers to the North and South from Each Defined Vent Site along the Ridge Axis

Vent	Latitude	Longitude	Depth (m)	Dispersal Distance (km)			
				1 Year (N)	1 Year (S)	6 Months (N)	6 Months (S)
1	38°22'48.0"N	30°36'36.0"W	1,319	13.11 (0.00–49.78)	90.84 (0.00–193.11)	0.00 (0.00–13.11)	25.79 (0.00–90.84)
MG	37°51'36.0"N	31°30'36.0"W	1,061	147.08 (31.11–147.08)	78.30 (12.50–78.30)	97.77 (8.80–147.08)	12.50 (0.00–78.30)
LS	37°17'24.0"N	32°19'12.0"W	1,855	49.28 (0.00–71.38)	44.41 (19.47–133.02)	0.00 (0.00–49.28)	44.41 (19.47–133.02)
2	36°53'24.0"N	33°10'12.0"W	2,233	37.88 (9.96–84.34)	22.24 (0.00–172.95)	25.95 (9.96–25.95)	16.10 (0.00–70.40)
RB	36°16'48.0"N	33°55'12.0"W	2,375	26.10 (26.10–104.81)	26.93 (0.00–103.02)	26.10 (8.98–85.94)	26.93 (0.00–26.93)
3	35°34'48.0"N	34°40'12.0"W	2,353	106.09 (10.09–109.16)	20.71 (20.71–278.10)	76.78 (10.09–103.02)	20.71 (0.00–20.71)
4	35°04'48.0"N	35°27'36.0"W	3,097	22.80 (22.80–22.80)	54.02 (13.39–228.17)	22.80 (22.80–22.80)	24.46 (13.39–54.02)
5	34°52'12.0"N	36°19'12.0"W	1,719	132.49 (23.74–148.91)	26.28 (9.98–110.45)	23.74 (23.74–132.49)	9.98 (0.00–110.45)
6	34°17'24.0"N	37°09'36.0"W	2,704	85.63 (26.62–199.02)	85.87 (0.00–408.45)	26.62 (26.62–199.02)	18.02 (0.00–105.77)
7	33°39'36.0"N	37°48'36.0"W	3,397	101.90 (52.88–118.31)	51.01 (0.00–166.92)	52.88 (29.24–92.15)	19.45 (0.00–121.52)
8	33°42'00.0"N	38°57'36.0"W	3,513	128.94 (28.17–178.71)	42.50 (0.00–120.94)	106.73 (28.17–128.94)	0.00 (0.00–106.55)
9	32°58'48.0"N	39°33'36.0"W	3,292	48.76 (23.49–134.81)	115.39 (59.61–147.64)	23.49 (23.49–23.49)	72.52 (23.50–147.64)
10	32°28'12.0"N	40°12'36.0"W	2,375	106.30 (10.91–247.10)	67.23 (67.23–67.23)	23.68 (10.91–168.96)	67.23 (67.23–67.23)
Median				85.63	51.01	25.95	20.71

Data are given as median values with range (minimum to maximum) for both 1-year and 6-month PLDs. Distances to the farthest measuring point are reported where observed dispersal probabilities were still >0. For each vent site, geographic coordinates and depth are given as used in the model. MG, Menez Gwen; LS, Lucky Strike; RB, Rainbow; 1–10, hypothetical vent sites (from north to south).

samples from MG, LS, and RB and samples from SP, IR, QS, and SM, because the required F_{ST} threshold of 0.05 was not met and runs with the unpooled dataset did not lead to consistent assignment results among replicates. Pooling effects were evaluated by running the program with only one population from each of the two pools.

Larval Dispersal Modeling

Larval trajectories from MG, LS, and RB were modeled with the particle-tracking routine Ariane [51] based on three-dimensional velocities produced by the North Atlantic OGCM VIKING20 [52] (Supplemental Experimental Procedures; Figures S1 and S2). Lagrangian simulations were performed for ~950,000 particles, released from each vent site during the natural spawning period between January and March [53] and passively drifting with the three-dimensional time-varying ocean velocities. To consider temporal fluctuations in current patterns, we modeled releases and dispersal between 1998 and 2007 assuming a typical PLD of 6 months [54] and a maximum PLD of 1 year [16]. Initial particle positions were determined with a power function that considered entrainment of larvae in rising hydrothermal plumes up to 400 mab [17] (Supplemental Experimental Procedures). After release, larvae were allowed to drift passively at any depth with the ocean currents, and no assumptions about mortality were made at any time of the simulations. Dispersal probabilities were computed as described previously [55]. To assess the probability of between-vent dispersal in relation to geographic distance, we positioned hypothetical suitable habitats along the ridge axis assuming vent occurrences every ~100 km [30]. For the calculations of dispersal kernels, only larvae that had been present within 400 mab during the dispersal period were considered. Point measurements of dispersal probabilities were taken ~10 km, ~25 km, and ~50 km to the north and south of each vent and were then measured every ~50 km along the MAR. Geographic distances and dispersal kernels were calculated and plotted with the *geosphere* and *ggplot2* packages in R v3.2.3 [56].

ACCESSION NUMBERS

The accession number for the raw RNA sequencing data is SRA: SRP076908. The accession numbers for the *ND4* sequences of the northern and southern Atlantic mussels reported in this paper are GenBank: KU950834–KU951111 and KX236334–KX236395. The DOI for the genotype, haplotype, and biophysical modeling data reported in this paper is PANGAEA: <https://doi.pangaea.de/10.1594/PANGAEA.860381>.

SUPPLEMENTAL INFORMATION

Supplemental Information includes Supplemental Experimental Procedures, two figures, and six tables and can be found with this article online at <http://dx.doi.org/10.1016/j.cub.2016.06.062>.

AUTHOR CONTRIBUTIONS

C.B. designed the study concept and performed the molecular biological, particle-tracking, and statistical analyses. A.B. provided the VIKING20 data and configured and supervised the larval dispersal simulations. A.D. validated the OGCM and produced the dispersal probability plots. A.M. supported the larval dispersal analyses and helped interpret the data. T.B. advised on sequencing design and transcriptome assembly and provided bioinformatics scripts. D.J. provided mussel samples and performed BLAST searches against the *B. azoricus* draft genome. L.S. reconstructed the *Bathymodiolus* endosymbiont genomes that supported the transcriptome assemblies. R.C.V., J.M.P., and N.D. contributed mussel samples and, together with F.M., provided advice on the data analyses and interpretation. M.B.S. and P.R. sequenced the *Bathymodiolus* transcriptomes. T.B.H.R. helped in developing the study concept and supervised the project. All authors contributed to the manuscript.

ACKNOWLEDGMENTS

We thank the ship captains, crews, and ROV pilots for their great efforts during sample collection, as well as Sven Petersen, François Lallier, and the IMAR/DOP University of the Azores for sharing mussel samples from the ODEMAR and BIOBAZ 2013 cruises (<http://dx.doi.org/10.17600/13030030>). Katrin Beining, Diana Gill, and Ulrike Panknin supported the laboratory work. Kiel University and the HLRN Hannover are acknowledged for giving access to their high-performance computing clusters. Melanie Vollstedt and Melanie Schlapkohl provided expert technical assistance with sequencing. We thank Erik Behrens for the VIKING20 model simulations and Patrick Wagner for the particle release scripts. Thanks to Oscar Puebla, David Haase, and Colin Devey for helpful discussions. The study was supported by C.B.'s and A.D.'s PhD studentships through the Helmholtz Research School on Ocean System Science and Technology (<http://www.hosst.org>) at GEOMAR Helmholtz Centre for Ocean Research Kiel (VH-KO-601) and Kiel University. L.S., J.M.P., and N.D. were

supported by the Max Planck Society, the MARUM at the University of Bremen, and an ERC Advanced Grant (BathyBiome, 340535).

Received: May 17, 2016

Revised: June 26, 2016

Accepted: June 28, 2016

Published: July 28, 2016

REFERENCES

- Ramirez-Llodra, E., Brandt, A., Danovaro, R., De Mol, B., Escobar, E., German, C.R., Levin, L.A., Martinez Arbizu, P., Menot, L., Buhl-Mortensen, P., et al. (2010). Deep, diverse and definitely different: unique attributes of the world's largest ecosystem. *Biogeosciences* 7, 2851–2899.
- Tivey, M. (2007). Generation of seafloor hydrothermal vent fluids and associated mineral deposits. *Oceanography (Wash. D.C.)* 20, 50–65.
- Dubilier, N., Bergin, C., and Lott, C. (2008). Symbiotic diversity in marine animals: the art of harnessing chemosynthesis. *Nat. Rev. Microbiol.* 6, 725–740.
- Marshall, D.J., Monro, K., Bode, M., Keough, M.J., and Swearer, S. (2010). Phenotype-environment mismatches reduce connectivity in the sea. *Ecol. Lett.* 13, 128–140.
- Gross, M. (2015). Deep sea in deep trouble? *Curr. Biol.* 25, R1019–R1021.
- Vrijenhoek, R.C. (2010). Genetic diversity and connectivity of deep-sea hydrothermal vent metapopulations. *Mol. Ecol.* 19, 4391–4411.
- Tyler, P.A., and Young, C.M. (1999). Reproduction and dispersal at vents and cold seeps. *J. Mar. Biol. Assoc. U. K.* 79, 193–208.
- Van Dover, C.L. (2014). Impacts of anthropogenic disturbances at deep-sea hydrothermal vent ecosystems: a review. *Mar. Environ. Res.* 102, 59–72.
- Adams, D., Arellano, S., and Govenar, B. (2012). Larval dispersal: vent life in the water column. *Oceanography (Wash. D.C.)* 25, 256–268.
- Cowen, R.K., and Sponaugle, S. (2009). Larval dispersal and marine population connectivity. *Annu. Rev. Mar. Sci.* 1, 443–466.
- Metaxas, A., and Saunders, M. (2009). Quantifying the “bio-” components in biophysical models of larval transport in marine benthic invertebrates: advances and pitfalls. *Biol. Bull.* 216, 257–272.
- Baltazar-Soares, M., Biastoch, A., Harrod, C., Hanel, R., Marohn, L., Prigge, E., Evans, D., Bodles, K., Behrens, E., Böning, C.W., and Eizaguirre, C. (2014). Recruitment collapse and population structure of the European eel shaped by local ocean current dynamics. *Curr. Biol.* 24, 104–108.
- Davies, S.W., Tremblay, E.A., Kenkel, C.D., and Matz, M.V. (2015). Exploring the role of Micronesian islands in the maintenance of coral genetic diversity in the Pacific Ocean. *Mol. Ecol.* 24, 70–82.
- Lukoschek, V., Riginos, C., and van Oppen, M.J. (2016). Congruent patterns of connectivity can inform management for broadcast spawning corals on the Great Barrier Reef. *Mol. Ecol.* 25, 3065–3080.
- Govenar, B. (2010). Shaping vent and seep communities: habitat provision and modification by foundation species. In *The Vent and Seep Biota*, S. Kiel, ed. (Springer), pp. 403–432.
- Arellano, S.M., and Young, C.M. (2009). Spawning, development, and the duration of larval life in a deep-sea cold-seep mussel. *Biol. Bull.* 216, 149–162.
- Mullineaux, L.S., Mills, S.W., Sweetman, A.K., Beaudreau, A.H., Metaxas, A., and Hunt, H.L. (2005). Vertical, lateral and temporal structure in larval distributions at hydrothermal vents. *Mar. Ecol. Prog. Ser.* 293, 1–16.
- Arellano, S.M., Van Gaest, A.L., Johnson, S.B., Vrijenhoek, R.C., and Young, C.M. (2014). Larvae from deep-sea methane seeps disperse in surface waters. *Proc. Biol. Sci.* 281, 20133276.
- Von Cosel, R., Comtet, T., and Krylova, E. (1999). *Bathymodiolus* (Bivalvia: Mytilidae) from hydrothermal vents on the Azores Triple Junction and the Logatchev Hydrothermal Field, Mid-Atlantic Ridge. *Veliger* 42, 218–248.
- van der Heijden, K., Petersen, J.M., Dubilier, N., and Borowski, C. (2012). Genetic connectivity between north and south Mid-Atlantic Ridge chemosynthetic bivalves and their symbionts. *PLoS ONE* 7, e39994.
- O'Mullan, G.D., Maas, P.A., Lutz, R.A., and Vrijenhoek, R.C. (2001). A hybrid zone between hydrothermal vent mussels (Bivalvia: Mytilidae) from the Mid-Atlantic Ridge. *Mol. Ecol.* 10, 2819–2831.
- Pritchard, J.K., Stephens, M., and Donnelly, P. (2000). Inference of population structure using multilocus genotype data. *Genetics* 155, 945–959.
- Evanno, G., Regnaut, S., and Goudet, J. (2005). Detecting the number of clusters of individuals using the software STRUCTURE: a simulation study. *Mol. Ecol.* 14, 2611–2620.
- Meirns, P.G. (2015). Seven common mistakes in population genetics and how to avoid them. *Mol. Ecol.* 24, 3223–3231.
- Wilson, G.A., and Rannala, B. (2003). Bayesian inference of recent migration rates using multilocus genotypes. *Genetics* 163, 1177–1191.
- Shanks, A.L. (2009). Pelagic larval duration and dispersal distance revisited. *Biol. Bull.* 216, 373–385.
- Rumrill, S.S. (1990). Natural mortality of marine invertebrate larvae. *Ophelia* 32, 163–198.
- Lenihan, H.S., Mills, S.W., Mullineaux, L.S., Peterson, C.H., Fisher, C.R., and Micheli, F. (2008). Biotic interactions at hydrothermal vents. Recruitment inhibition by the mussel *Bathymodiolus thermophilus*. *Deep Sea Res. Part I Oceanogr. Res. Pap.* 55, 1707–1717.
- Arellano, S.M. (2008). Embryology, larval ecology, and recruitment of “*Bathymodiolus*” *childressi*, a cold-seep mussel from the Gulf of Mexico. PhD dissertation. (University of Oregon).
- Beaulieu, S.E., Baker, E.T., and German, C.R. (2015). Where are the undiscovered hydrothermal vents on oceanic spreading ridges? *Deep Sea Res. Part II Top. Stud. Oceanogr.* 121, 202–212.
- Baker, E.T., Resing, J.A., Haymon, R.M., Tunnicliffe, V., Lavelle, J.W., Martinez, F., Ferrini, V., Walker, S.L., and Nakamura, K. (2016). How many vent fields? New estimates of vent field populations on ocean ridges from precise mapping of hydrothermal discharge locations. *Earth Planet. Sci. Lett.* 449, 186–196.
- DeChaine, E.G., Bates, A.E., Shank, T.M., and Cavanaugh, C.M. (2006). Off-axis symbiosis found: characterization and biogeography of bacterial symbionts of *Bathymodiolus* mussels from Lost City hydrothermal vents. *Environ. Microbiol.* 8, 1902–1912.
- Mitarai, S., Watanabe, H., Nakajima, Y., Shchepetkin, A.F., and McWilliams, J.C. (2016). Quantifying dispersal from hydrothermal vent fields in the western Pacific Ocean. *Proc. Natl. Acad. Sci. USA* 113, 2976–2981.
- Morato, T., Cleary, J., Taranto, G.H., Vandeperre, F., Pham, C.K., Dunn, D.C., Colaço, A., and Halpin, P.N. (2015). Data Report: Towards Development of a Strategic Environmental Management Plan for Deep Seabed Mineral Exploitation in the Atlantic Basin (IMAR and MGEL).
- Hilário, A., Metaxas, A., Gaudron, S.M., Howell, K.L., Mercier, A., Mestre, N.C., Ross, R.E., Thurnherr, A.M., and Young, C. (2015). Estimating dispersal distance in the deep sea: challenges and applications to marine reserves. *Front. Mar. Sci.* 2, 20133276.
- Young, C.M., He, R., Emler, R.B., Li, Y., Qian, H., Arellano, S.M., Van Gaest, A., Bennett, K.C., Wolf, M., Smart, T.I., and Rice, M.E. (2012). Dispersal of deep-sea larvae from the intra-American seas: simulations of trajectories using ocean models. *Integr. Comp. Biol.* 52, 483–496.
- Chevaldonné, P., Jollivet, D., Vangriesheim, A., and Desbruyères, D. (1997). Hydrothermal-vent alvinellid polychaete dispersal in the eastern Pacific. 1. Influence of vent site distribution, bottom currents, and biological patterns. *Limnol. Oceanogr.* 42, 67–80.
- Boschen, R.E., Collins, P.C., Tunnicliffe, V., Carlsson, J., Gardner, J.P.A., Lowe, J., McCrone, A., Metaxas, A., Sinniger, F., and Swadlow, A. (2016). A primer for use of genetic tools in selecting and testing the suitability of

- set-aside sites protected from deep-sea seafloor massive sulfide mining activities. *Ocean Coast. Manage.* 122, 37–48.
39. Dodt, M., Roehr, J.T., Ahmed, R., and Dieterich, C. (2012). FLEXBAR—flexible barcode and adapter processing for next-generation sequencing platforms. *Biology (Basel)* 1, 895–905.
 40. Grabherr, M.G., Haas, B.J., Yassour, M., Levin, J.Z., Thompson, D.A., Amit, I., Adiconis, X., Fan, L., Raychowdhury, R., Zeng, Q., et al. (2011). Full-length transcriptome assembly from RNA-seq data without a reference genome. *Nat. Biotechnol.* 29, 644–652.
 41. Li, W., and Godzik, A. (2006). Cd-hit: a fast program for clustering and comparing large sets of protein or nucleotide sequences. *Bioinformatics* 22, 1658–1659.
 42. Koboldt, D.C., Zhang, Q., Larson, D.E., Shen, D., McLellan, M.D., Lin, L., Miller, C.A., Mardis, E.R., Ding, L., and Wilson, R.K. (2012). VarScan 2: somatic mutation and copy number alteration discovery in cancer by exome sequencing. *Genome Res.* 22, 568–576.
 43. Tsagkogeorga, G., Cahais, V., and Galtier, N. (2012). The population genomics of a fast evolver: high levels of diversity, functional constraint, and molecular adaptation in the tunicate *Ciona intestinalis*. *Genome Biol. Evol.* 4, 740–749.
 44. Benson, G. (1999). Tandem repeats finder: a program to analyze DNA sequences. *Nucleic Acids Res.* 27, 573–580.
 45. Guichoux, E., Lagache, L., Wagner, S., Chaumeil, P., Léger, P., Lepais, O., Lepoittevin, C., Malausa, T., Revardel, E., Salin, F., and Petit, R.J. (2011). Current trends in microsatellite genotyping. *Mol. Ecol. Resour.* 11, 591–611.
 46. Altschul, S.F., Gish, W., Miller, W., Myers, E.W., and Lipman, D.J. (1990). Basic local alignment search tool. *J. Mol. Biol.* 215, 403–410.
 47. Untergasser, A., Cutcutache, I., Koressaar, T., Ye, J., Faircloth, B.C., Remm, M., and Rozen, S.G. (2012). Primer3—new capabilities and interfaces. *Nucleic Acids Res.* 40, e115.
 48. Excoffier, L., and Lischer, H.E.L. (2010). Arlequin suite ver 3.5: a new series of programs to perform population genetics analyses under Linux and Windows. *Mol. Ecol. Resour.* 10, 564–567.
 49. Foll, M., and Gaggiotti, O. (2008). A genome-scan method to identify selected loci appropriate for both dominant and codominant markers: a Bayesian perspective. *Genetics* 180, 977–993.
 50. Breusing, C., Johnson, S.B., Tunnicliffe, V., and Vrijenhoek, R.C. (2015). Population structure and connectivity in Indo-Pacific deep-sea mussels of the *Bathymodiolus septemdirum* complex. *Conserv. Genet.* 16, 1415–1430.
 51. Blanke, B., Arhan, M., Madec, G., and Roche, S. (1999). Warm water paths in the equatorial Atlantic as diagnosed with a general circulation model. *J. Phys. Oceanogr.* 29, 2753–2768.
 52. Böning, C.W., Behrens, E., Biastoch, A., and Bamber, J.L. (2016). Emerging impact of Greenland meltwater on deepwater formation in the North Atlantic Ocean. *Nat. Geosci.* 9, 523–527.
 53. Colaço, A., Martins, I., Laranjo, M., Pires, L., Leal, C., Prieto, C., Costa, V., Lopes, H., Rosa, D., Dando, P.R., and Serrão-Santos, R. (2006). Annual spawning of the hydrothermal vent mussel, *Bathymodiolus azoricus*, under controlled aquarium, conditions at atmospheric pressure. *J. Exp. Mar. Biol. Ecol.* 333, 166–171.
 54. Dixon, D.R., Lowe, D.M., Miller, P.I., Villemin, G.R., Colaço, A., Serrão-Santos, R., and Dixon, L.R.J. (2006). Evidence of seasonal reproduction in the Atlantic vent mussel *Bathymodiolus azoricus*, and an apparent link with the timing of photosynthetic primary production. *J. Mar. Biol. Assoc. U. K.* 86, 1363–1371.
 55. Gary, S.F., Lozier, M.S., Biastoch, A., and Böning, C.W. (2012). Reconciling tracer and float observations of the export pathways of Labrador Sea Water. *Geophys. Res. Lett.* 39, L24606.
 56. R Development Core Team (2015). R: a language and environment for statistical computing (R Foundation for Statistical Computing).